

Electrochemical performance of LAGP based polymer electrolyte for solid-state battery application

A. Das^{1,2}, M. Goswami^{1,2*}

¹Glass & Advanced Materials Division, Bhabha Atomic Research Centre, Trombay, Mumbai 400085, India

²Homi Bhabha National Institute, Anushaktinagar, Mumbai 400094, India

Accepted: July 06, 2022

To address the safety issues of the commercial lithium ion batteries, composite solid electrolytes (CSEs) are promising alternatives. Fabrication of micron-size thin pure solid state electrolyte (SSE) is difficult. It can be solved by incorporating active filler (SSE) into the polymer. In this work we report synthesis of a CSE by incorporating LAGP ($\text{Li}_2\text{O}-\text{Al}_2\text{O}_3-\text{GeO}_2-\text{P}_2\text{O}_5$) (SSE), LiTFSI, EMIMTFSI into PVDF-HFP polymer. Cyclic voltammetry experiment of Li/CSE/LFP (LiFePO_4) showed only two broad peaks at 3.8 V and 3.1 V for oxidation and reduction of lithium, respectively. The value of transference number obtained from a symmetric cell study is 0.16. The galvanostatic charge/discharge profiles of the fabricated solid state cell were recorded at C/15. The value of discharge capacity was 150 mAhg^{-1} (88% of theoretical capacity) which was almost constant up to the 40th cycle.

Keywords: Glass ceramics; solid state battery; solid state electrolyte; NASICON; LAGP

INTRODUCTION

Lithium ion batteries (LIBs) are being widely used in recent years for their applications as energy storage device in various electronic gadgets. However, LIBs suffer with various shortcomings: (a) internal short circuit (b) fire or explosion at high temperature because of the uses of a flammable liquid electrolyte, etc. [1]. To avoid all these issues pertaining to conventional LIBs, ASSLBs (all solid state lithium batteries) are recognized as the safest alternative [2]. ASSLBs have mainly three components: cathode, anode and solid-state-electrolyte (SSE). The charging and discharging mechanism is the same as for LIBs. Lithium ion is transferred from cathode to anode through SSE while charging and during the discharge process the exactly reverse phenomenon takes place [3]. SSEs are mainly two types: organic and inorganic. Despite several advantages of organic SSE, it has few drawbacks like narrow temperature range and poor structural stability, whereas inorganic SSEs can have improved stability and safety over a wide temperature range. A promising SSE should have high ionic conductivity, thermal and electrochemical stability. Lithium ions hop from one stable position to another inside the SSE. Therefore, the ion diffusion is mainly related to the crystal lattice of the SSE. The ion migration channel can be widened by doping. Among other inorganic SSEs, oxide SSEs are more environment-friendly and can be easily processed. These kind of materials are mainly polycrystalline, where the lithium ion migrates through two regions:

grain and grain boundary. The movement is slow inside the grain boundary as compared to the grain. Therefore, the oxide SSEs should have large and dense grains [4]. Among other oxides (i.e. perovskite, garnet, etc.) Li-based NASICON (Na super-ionic conductor) type materials ($\text{LiM}^{(\text{IV})}_2(\text{PO}_4)_3$, $\text{M}^{(\text{IV})}$: Ge^{4+} , Ti^{4+} , Zr^{4+} , etc.) with high ionic mobility show a potential application in ASSLBs as SSE [5]. Again, due to high interfacial resistance between rigid polycrystalline SSE and the electrode, modifications are required by mixing with polymer [6].

In this study glass ceramics-based NASICON type $\text{Li}_{1.5}\text{Al}_{0.5}\text{Ge}_{1.5}\text{P}_{2.9}\text{Si}_{0.1}\text{O}_{12}$ (LAGP) SSE was prepared. To enhance the electrochemical stability, the composite solid electrolyte (CSE) was synthesized by incorporating PVDF-HFP, lithium bis(tri-fluoromethanesulfonyl) imide (LiTFSI) and 1-ethyl-3-methylimidazolium bis(trifluoromethyl sulfonyl) imide (EMITFSI). To ensure the lithium ion insertion/extraction reaction a cyclic voltammetry (CV) experiment was carried out. Lithium ion transference number was estimated using d.c. polarization experiment along with complex impedance spectroscopy (CIS). Automatic battery analyzer was used to study the cell performance.

EXPERIMENTAL

Preparation of LAGP glass & glass-ceramics

Glass with composition $\text{Li}_{1.5}\text{Al}_{0.5}\text{Ge}_{1.5}\text{P}_{2.9}\text{Si}_{0.1}\text{O}_{12}$ (LAGP) was prepared using conventional melt-

* To whom all correspondence should be sent:
E-mail:mgoswami@barc.gov.in

quenching technique. The purity of the constituent chemicals was 99.9% or higher. The batch was prepared in weight of 100 g. Calcination was performed after thorough mixing of the initial components. This process was repeated for complete decomposition of the initial constituents to the corresponding oxide forms. After that, the powder was taken in a Pt-Rh crucible and the latter was put inside a furnace at 1500°C for melting. Melt was kept at that temperature for sufficient time to ensure complete melting and finally cast into a pre-heated graphite mold. Prepared glass sample was annealed at 500°C for 4 h. LAGP glass-ceramics sample was prepared using optimized heat treatment based on DTA data.

Composite solid electrolyte (CSE) synthesis

PVDF-HFP + 20wt.% LAGP + 20wt.% LiTFSI + 35wt.% EMITFSI were mixed to prepare CSE by the solution casting method. In this technique, appropriate proportion of PVDF-HFP was dissolved in acetone under constant stirring at 100 rpm at 50°C for 3-4 hours to get crystal clear solution. Then, LiTFSI and EMITFSI were added to the solution and stirred magnetically for 2 hours. After that, LAGP powder was mixed with the solution and stirred for 20 hours for homogeneous mixing. Then the solution was cast on a glass plate and dried in ambient conditions for 3-4 days. Finally, the thin and flexible CSE film was peeled off from the glass surface and was dried in an oven at 50°C overnight. The thickness of the CSE obtained was 100-150 μm. The sample was transferred into a Ar-filled glove box for future studies.

Electrode preparation

LiFePO₄ (LFP) was used as active cathode material. For preparation of cathode, a slurry of 40wt.% LFP, 55 wt.% CSE and 5 wt.% carbon black was prepared using NMP as dispersant instead of acetone used for CSE preparation. Here, PVDF was used as a binder polymer. Film coater was used to coat the slurry onto an aluminium foil. After that, the coating was dried overnight at 60°C inside an oven. Then the cathode was cut into 1cm×1cm square pieces and kept inside the glove box. The amount of active material in the cathode was 2.86gcm⁻². The anode material was lithium metal. Before the cell fabrication the oxidised layer on the lithium foil was cleaned using hexane.

Cell fabrication

The cell was prepared by sandwiching CSE between prepared cathode and lithium metal anode inside the glove box. Automatic crimper and

CR2032 coin cell were used for cell fabrication. The cell was kept overnight for stabilization.

Experimentation

Lithium ion transference number and cyclic voltammetry (CV) experiments were performed using Advanced Electrochemical System (PARSTAT 2273, Princeton Applied Research) at a scan rate of 0.1 Vsec⁻¹ from 2.7 V to 4.2 V. NOVO Control Impedance analyzer was used for ac impedance measurements. The lithium ion transference number (t_{Li^+}) of the CSE was evaluated using combined ac/dc technique. A dc volt of 5m V was applied on Li|CSE|Li symmetric cell for 2 hours for polarization and the corresponding current was measured. The cell resistance was also measured before and after polarization using complex impedance spectroscopy. The value of t_{Li^+} was calculated using Bruce-Vincent's equation:

$$t_{Li^+} = \dots \quad (1)$$

where, ΔV is the applied small constant dc potential, I_0 and R_0 are the current and resistance before polarization, I_{SS} and R_{SS} are the current and resistance after polarization (or at steady state) [7]. Galvanostatic charge/discharge experiments were carried out within the voltage range of 2.7-4.0 V at room temperature using Neware automatic battery analyzer.

RESULTS AND DISCUSSION

Fig. 1. shows the CV curves of Li|CSE|LFP solid state cell at room temperature. Two broad peaks were observed at 3.2 and 3.8 V vs Li/Li⁺ due to lithium ion insertion and extraction, respectively [8]. There is no other peak found in the scans, which indicates the absence of any other side reaction within this voltage range.

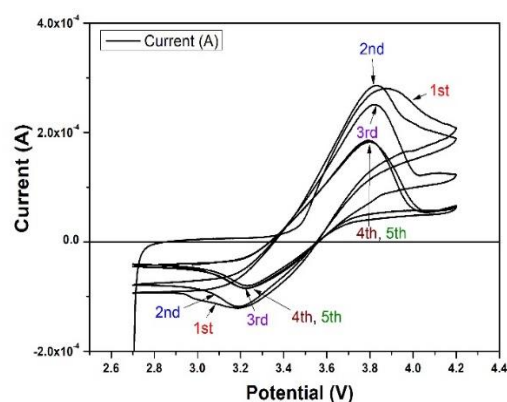


Fig. 1. CV scans of Li|CSE|LFP cell

After 4 cycles the peak current became steady. Amplitudes of the anodic and cathodic peaks are not

equal indicating that the diffusion behavior is not the same inside the cathode (LFP) and anode (lithium metal). Guo *et al.* also reported this kind of CV plot at room temperature [9].

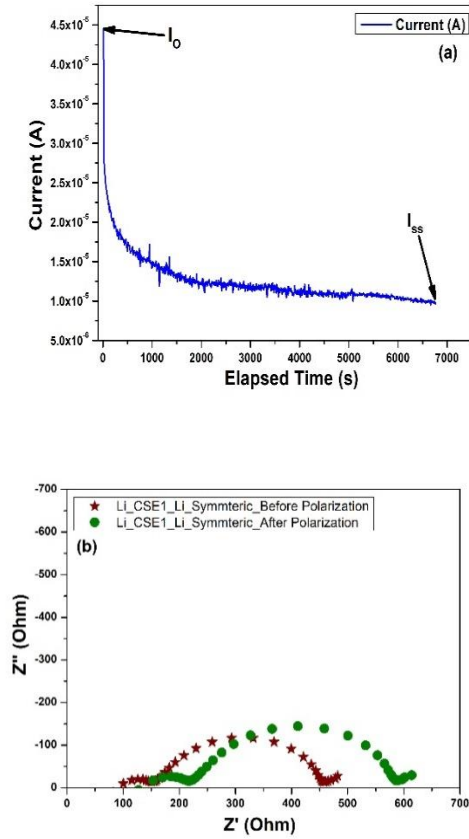


Fig. 2. (a) DC polarization curve of Li|CSE|Li symmetric cell at a fixed applied voltage. (b) AC impedance plot of the symmetric cell before and after polarization

Polarization current *versus* time plot of the symmetric cell (Li|CSE|Li) is shown in Fig. 2(a). After applying a constant voltage (ΔV) across the cell, ions move towards the electrode/electrolyte interface and start to accumulate there. This causes a current flow (I_0) initially as seen in Fig. 2(a). Ions are getting accumulated at the lithium metal surface and form a space charge region which reduces the polarization current with time [10]. Since the ions are getting absorbed at the lithium metal surface, the final current can be designated as a steady state current (I_{ss}) due to only lithium ions movement. Fig. 2(b) shows the complex impedance plot of the Li|CSE|Li cell before and after the d.c. polarization experiment. The small semicircular part in the high frequency region represents the bulk resistance of the CSE, while the mid frequency intercept indicates the combined effect of interfacial, charge-transfer and passive layer resistances. The lithium ion

transference number (t_{Li^+}) (Table 1) was estimated using equation 1, where total resistance, R_0 and R_{ss} , was computed before and after d.c. polarization, respectively. Similar values of t_{Li^+} are reported in the literature [11,12]. Hence, the value of 0.16 is sufficient to use as a solid electrolyte inside a lithium ion cell.

Table 1. Evaluation of t_{Li^+}

ΔV (V)	R_0 (Ω)	I_0 (μA)	R_{ss} (Ω)	I_{ss} (μA)	t_{Li^+}
0.05V	454	44	587	10	0.16

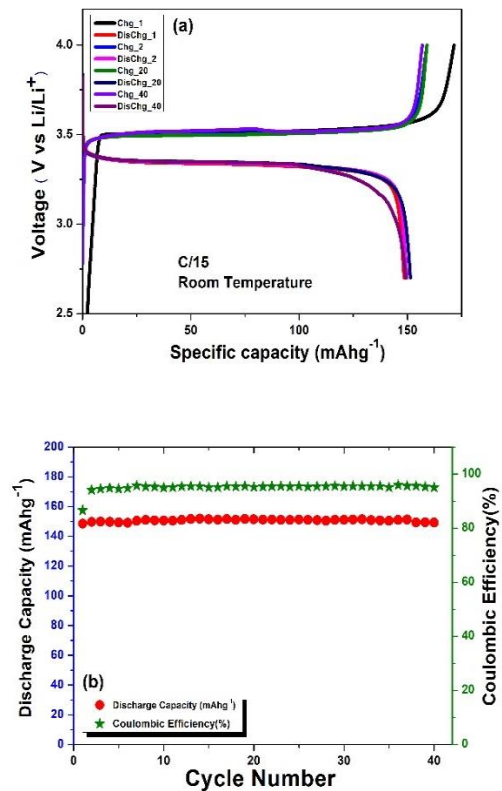


Fig. 3. (a) Galvanostatic charge/discharge profiles (b) Specific discharge capacity and coulombic efficiency, of Li|CSE|LFP solid state cell.

Fig. 3(a) shows the galvanostatic charge/discharge profiles of the cell Li|CSE|LFP at C/15 current rate ($1C=170 \text{ mA g}^{-1}$) within 2.7 to 4.0 V vs. Li/Li⁺. The average voltage plateaux of charging and discharging curves are 3.50 and 3.34 V, respectively. The polarization obtained from Fig. 3(a) is around 0.16 V, which arises because of the interfacial, as well as the charge transfer resistance. Specific discharge capacity and coulombic efficiency are shown in Fig. 3(b) up to 40 cycles at C/15 rate. Specific discharge capacity of the solid state cell is $\sim 150 \text{ mAhg}^{-1}$ and this value is higher than the previously reported values for the similar

A. Das, M. Goswami: *Electrochemical performance of LAGP based polymer electrolyte for solid-state-battery...* composite solid electrolytes at room temperature [9, 13]. A stable coulombic efficiency of ~95% was observed up to 40 cycles except for the first cycle due to formation of a stable solid electrolyte interface (SEI) layer.

CONCLUSIONS

In this study LAGP based composite solid electrolyte (CSE) was prepared using PVDF-HFP, LiTFSI and EMITFSI. Cyclic voltammetry study revealed successful lithium intercalation/de-intercalation by indicating broad anodic and cathodic peaks. No other peak in the CV scans confirms that there was no side reaction. Lithium ion transference number (t_{Li^+}) was obtained ~0.16 which is comparable to solid-state electrolytes. The fabricated solid-state cell (Li|CSE|LFP) exhibited good capacity retention and delivered 88% of the theoretical capacity (170 mAhg^{-1}). It also showed stable coulombic efficiency up to 40 cycles of charge/discharge.

REFERENCES

1. N. Kamaya, K. Homma, Y. Yamakawa, M. Hirayama, R. Kanno, M. Yonemura, T. Kamiyama, Y. Kato, S. Hama, K. Kawamoto, A. Mitsui, *Nat. Mater.*, **10**, 682 (2011).
2. M. Tatsumisago, M. Nagao, A. Hayashi, *J. Asian Ceram. Soc.*, **1**, 17 (2013).
3. B. Scrosati, G. Jürgen, *J. Power Sources*, **195**, 2419 (2010).
4. X. Yao, B. Huang, J. Yin, G. Peng, X. Xu, *Chin. Phys. B*, **25**, 018802 (2016).
5. L. Shi-Chun, L. Zu-Xiang, *Solid State Ion.*, **10**, 835 (1983).
6. A. Das, M. Goswami, P. Preetham, S. K. Deshpande, S. Mitra, M. Krishnan, Springer Conference Proceedings., doi:10.1007/978-981-15-5955-6_23.
7. Y. lin, J. Li, Y. Lai, C. Yuan, Y. Cheng, J. Liu, *RSC Adv.*, **3**, 10722 (2013).
8. H. Gupta, S. Kataria, L. Balo, V. K. Singh, S. K. Singh, A. K. Tripathi, Y. L. Verma, R. K. Singh, *Solid State Ion.*, **320**, 186 (2018).
9. Q. Guo, Y. Han, H. Wang, S. Xiong, W. Sun, C. Zheng, K. Xie, *Electrochim. Acta*, **296**, 693 (2019).
10. H. Cheng, C. B. Zhu, B. Huang, M. Lu, Y. Yang, *Electrochim. Acta*, **52**, 5789 (2007).
11. L. Balo, H. Gupta, S. K. Singh, V. K. Singh, S. Kataria, R. K. Singh, *J. Ind. Eng. Chem.*, **65**, 137 (2018).
12. S. K. Singh, D. Dutta, R. K. Singh, *Electrochim. Acta*, **343**, 136122 (2020).
13. Q. Guo, Y. Han, H. Wang, S. Xiong, W. Sun, C. Zheng, K. Xie, *J. Phys. Chem. C*, **122**, 10334 (2018).